Wide-Band Strip-Line Magic-T*

E. M. T. JONES†

Summary—**This paper presents theoretical performance calculations of a novel form of wide-band strip-line Magic-T that uses two dual strip-line band-pass filters. When all four ports are terminated in the same impedance, the VSWR at each port is less than 1.47 over a 2:1 frequency band, while the isolation between opposite ports is greater than 20 db over this frequency band.**

Introduction

THE fundamental characteristics of distributed-circuit hybrids, which function as Magic-T's, were described by Tyrell[1] in 1947. Since that time, a number of workers have described the performance of practical wide-band realizations constructed in coaxial line[2–5] and strip line.[5] The best reported performance of these Magic-T's was obtained by Alford and Watts,[5] who quote for their coaxial-line model, operating from 100 to 200 mc, isolations of greater than 45 db and VSWR's of less than 1.4 at any port.

This paper contains a theoretical analysis of a new type of wide-band strip-line Magic-T. A schematic diagram of this device is shown in Fig. 1. It is seen that ports 4 and 3 and ports 4 and 2 are connected by means of transmission lines of characteristic impedance Z and electrical length θ. Port 1 is connected to port 2 by means of a band-pass filter[6] having image impedance Z_o[7] and image phase shift β, while port 1 is connected to port 3 by a band-pass filter which is the dual of that connecting ports 1 and 2. It has image impedance Z_s and an image phase shift $\beta+180$ degrees. The definitions[6] of these quantities are

$$Z_s = \frac{2Z_{oe}Z_{oo}\sin\theta}{[(Z_{oe}-Z_{oo})^2-(Z_{oe}+Z_{oo})^2\cos^2\theta]^{1/2}},\text{ or, the}$$

image impedance of the filter with the pair of shorted strips.

Z_{oe} = Characteristic impedance of one coupled strip, measured with respect to ground, with equal currents flowing in the same direction.

Z_{oo} = Characteristic impedance of one coupled strip, measured with respect to ground, with equal currents flowing in opposite directions.

$Z_o = Z_{oe}Z_{oo}/Z_s$, or, the image impedance of the filter with the pair of open-circuited strips.

θ = Electrical length of each band-pass filter and each line of characteristic impedance Z.

$$\beta = \cos^{-1}\left[\frac{(Z_{oe}+Z_{oo})}{(Z_{oe}-Z_{oo})}\cos\theta\right]\text{ image phase shift of}$$

the filter with the pair of open-circuited strips.

$\beta+180°$ = Image phase shift of the filter with the pair of short-circuited strips.

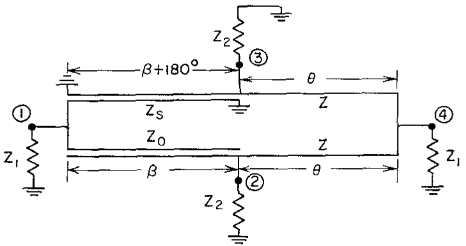

Fig. 1—Schematic diagram of a wide-band strip-line magic-T.

At midband, where $\theta=90°$, it is seen that β is always equal to 90° for arbitrary values of Z_{oe} and Z_{oo}. If one chooses Z_{oe} and Z_{oo} as

$$\begin{aligned} Z_{oe} &= Z(\sqrt{2}+1) \\ Z_{oo} &= Z(\sqrt{2}-1) \end{aligned} \tag{1}$$

then, $Z_o=Z_s=Z$ at midband. If, in addition, the values of the four terminating impedances satisfy the relation

$$2Z_1 = Z_2 = Z \tag{2}$$

then the Magic-T is perfectly matched at midband at all ports and, hence, has perfect midband isolation between ports 1 and 4, and ports 2 and 3. Inspection of Fig. 1 shows that ports 2 and 3 are equivalent to the through arms of a waveguide Magic-T while ports 1 and 4 are equivalent to the ports on the series and shunt arms, respectively, of a waveguide Magic-T. At frequencies other than the midband frequency, the various ports will not be perfectly matched and the isolation

* Manuscript received by the PGMTT, September 2, 1959. The work described in this paper was sponsored by the USASRDL under Contract DA 36-039 SC-74862.

† Stanford Research Institute, Menlo Park, Calif.

[1] W. A. Tyrell, "Hybrid circuits for microwaves," Proc. IRE, vol. 35, pp. 1294–1306; November, 1947.

[2] T. Morita and L. S. Sheingold, "A coaxial Magic-T," IRE Trans. on Microwave Theory and Techniques, vol. 1, pp. 17–23; November, 1953.

[3] V. I. Albanese and W. P. Peyser, "An analysis of a broad-band coaxial hybrid ring," IRE Trans. on Microwave Theory and Techniques, vol. 6, pp. 369–373; October, 1958.

[4] W. V. Tyminski and A. E. Hylas, "A wide-band hybrid ring for UHF," Proc. IRE, vol. 41, pp. 81–87; January, 1953.

[5] A. Alford and C. B. Watts, "A wide-band coaxial hybrid," 1956 IRE National Convention Record, Pt. I, pp. 171–179.

[6] E. M. T. Jones and J. T. Bolljahn, "Coupled-strip-transmission-line filters and directional coupler," IRE Trans. on Microwave Theory and Techniques, vol. 4, pp. 75–81; April, 1956.

[7] The subscript s applies to the filter with the pair of short-circuited strips, while the subscript o applies to the filter with the pair of open-circuited strips.

between opposite ports will not be infinite. Nevertheless, as will be shown later, the calculated performance of this Magic-T is quite good over a 2:1 frequency band. Calculations are also presented for cases when the various impedances are different from those defined by (1) and (2). It is shown that optimum performance over the 2:1 frequency band is obtained when $Z_1/Z=Z_2/Z=0.8024$ and $Z_o/Z=1.0785$ at midband.

The performance of these Magic-T's as a function of frequency is analyzed here in terms of the well-known $ABCD$ matrices of the individual networks within a particular Magic-T. These matrices are listed in Table I for reference.

TABLE I
ABCD MATRICES OF THE INDIVIDUAL NETWORKS IN THE MAGIC-T

Network	Matrix
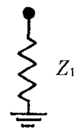	$\begin{vmatrix} 1 & 0 \\ \frac{1}{Z_1} & 1 \end{vmatrix} = \lvert M_1 \rvert$
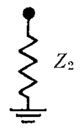	$\begin{vmatrix} 1 & 0 \\ \frac{1}{Z_2} & 1 \end{vmatrix} = \lvert M_2 \rvert$
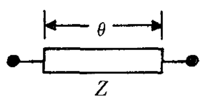	$\begin{vmatrix} \cos\theta & jZ\sin\theta \\ j\frac{\sin\theta}{Z} & \cos\theta \end{vmatrix} = \lvert M_3 \rvert$
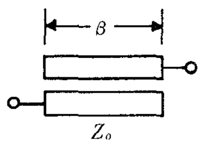	$\begin{vmatrix} \cos\beta & +jZ_o\sin\beta \\ j\frac{\sin\beta}{Z_o} & \cos\beta \end{vmatrix} = \lvert M_4 \rvert$
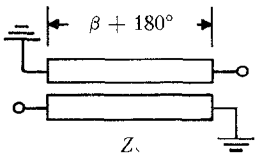	$\begin{vmatrix} -\cos\beta & -jZ_o\sin\beta \\ -j\frac{\sin\beta}{Z_o} & -\cos\beta \end{vmatrix} = \lvert M_5 \rvert$

The techniques used to compute the input impedance of any port and the output voltages at the other ports will now be illustrated for the case when port 1 is energized. Fig. 2 shows the Magic-T of Fig. 1 redrawn in a convenient form for computation of the input impedance of port 1 and the isolation between ports 1 and 4.

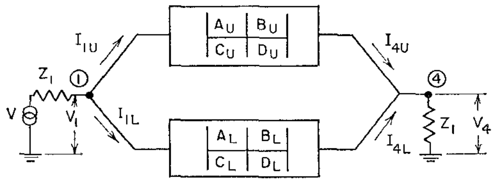

Fig. 2—Magic-T equivalent circuit used in computing voltages at ports 1 and 4.

Here the matrix elements of the upper network are given by

$$\begin{vmatrix} A_U & B_U \\ C_U & D_U \end{vmatrix} = \lvert M_5 \rvert \times \lvert M_2 \rvert \times \lvert M_3 \rvert, \quad (3)$$

while those in the lower network are given by

$$\begin{vmatrix} A_L & B_L \\ C_L & D_L \end{vmatrix} = \lvert M_4 \rvert \times \lvert M_2 \rvert \times \lvert M_3 \rvert. \quad (4)$$

The voltages and currents at the two ports are related by

$$V_1 = A_U V_4 + B_U I_{4U}$$
$$I_{1U} = C_U V_4 + D_U I_{4U} \quad (5)$$

and

$$V_1 = A_L V_4 + B_L I_{4L}$$
$$I_{1L} = C_L V_4 + D_L I_{4L}. \quad (6)$$

The currents I_{4U} and I_{4L} are related as

$$(I_{4U} + I_{4L})Z_1 = V_4. \quad (7)$$

When (7) is substituted into (6) and (5), one finds that the input impedance $Z_{\text{in}(1)}$ at port 1 is

$$Z_{\text{in}(1)} = \frac{V_1}{I_{1U}+I_{1L}} = \frac{A_U B_L + B_U A_L + \frac{B_U B_L}{Z_1}}{-2 + B_U C_L + B_L C_U + D_U A_L + D_L A_U + \frac{B_U D_L + D_U B_L}{Z_1}}. \quad (8)$$

The input impedance at port 4 when port 1 is terminated in Z_1 is easily determined by replacing, in (8), A_U by D_U, D_U by A_U, A_L by D_L, and D_L by A_L.

It is easy to show that the ratio of V_1/V_4 when port 1 is energized is given as

$$\frac{V_1}{V_4} = \frac{\dfrac{B_U B_L}{Z_1} + A_U B_L + A_L B_U}{B_L + B_U}. \tag{9}$$

The ratio V_4/V_1 when port 4 is energized is determined by replacing, in (9), A_U by D_U and A_L by D_L, which shows that in general these ratios are slightly different. The actual insertion loss, *I.L.*, between ports 1 and 4, is independent of the direction of propagation through the network and is given by

$$I.L. = \left[\frac{1}{|1+\Gamma_{in(1)}|}\,\frac{\dfrac{B_U B_L}{Z_1} + A_U B_L + A_L B_U}{B_L + B_U}\right]^2 \tag{10}$$

or

$$I.L. = \left[\frac{1}{|1+\Gamma_{in(4)}|}\,\frac{\dfrac{B_U B_L}{Z_1} + D_U B_L + D_L B_U}{B_L + B_U}\right]^2,$$

where

$$\Gamma_{in(1)} = \frac{Z_{in}(1) - Z_1}{Z_{in}(1) + Z_1}$$

$$\Gamma_{in(4)} = \frac{Z_{in}(4) - Z_1}{Z_{in}(4) + Z_1}.$$

Eq. (10) predicts that the insertion loss between ports 1 and 4 is infinite only when $Z_s = Z_o = Z$.

The voltage at port 3 when port 1 is energized is determined with the aid of the circuit in Fig. 3. The matrices in this circuit have the values

$$\begin{vmatrix} A' & B' \\ C' & D' \end{vmatrix} = |M_4| \times |M_2| \times |M_3| \times |M_1| \times |M_3| \tag{11}$$

and

$$\begin{vmatrix} A_5 & B_5 \\ C_5 & D_5 \end{vmatrix} = M_5.$$

The voltage ratio V_3/V_1 is

$$\frac{V_3}{V_1} = \frac{B' + B_5}{\dfrac{B'B_5}{Z_2} + A'B_5 + A_5 B'}. \tag{12}$$

The voltage at port 2 when port 1 is energized is determined with the aid of Fig. 4. The matrices in this circuit have the values

$$\begin{vmatrix} A'' & B'' \\ C'' & D'' \end{vmatrix} = |M_5| \times |M_2| \times |M_3| \times |M_1| \times |M_3|, \tag{13}$$

and

$$\begin{vmatrix} A_4 & B_4 \\ C_4 & D_4 \end{vmatrix} = |M_4|.$$

The voltage ratio V_2/V_1 is

$$\frac{V_2}{V_1} = \frac{B'' + B_4}{\dfrac{B'B_4}{Z_2} + A''B_4 + A_4 B''}. \tag{14}$$

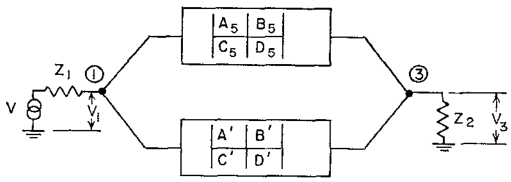

Fig. 3—Magic-T equivalent circuit used in computing voltages at ports 1 and 3.

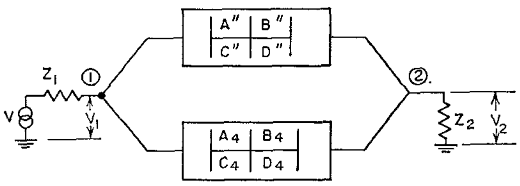

Fig. 4—Magic-T equivalent circuit used in computing voltages at ports 1 and 2.

The input impedance of the other ports and the voltage transfer coefficients between the various ports when a particular port is energized may be written by inspection using the above technique. One interesting result of such a procedure is the fact that the insertion loss between ports 2 and 3 is infinite only when $Z_s Z_o = Z^2$ and $\theta = \beta = 90°$. This condition is satisfied at midband for all the Magic-T's discussed here.

The electrical performances of five Magic-T's have been computed on a high-speed digital computer using the above formulas. The important electrical parameters of these structures are listed in Table II. The input impedance at the four ports of these Magic-T's are plotted in Figs. 5 through 9. It is observed that in all cases the real part of the input impedance of a port is a symmetrical function of frequency while the imaginary part is an antisymmetrical function of frequency. Furthermore, the input impedance at each of the various ports of any one Magic-T has a different variation with fre-

TABLE II
ELECTRICAL PARAMETERS OF VARIOUS STRIP-LINE MAGIC-T'S

	Magic-T Number 1	Magic-T Number 2	Magic-T Number 3	Magic-T Number 4	Magic-T Number 5
Z_{oe}/Z	2.414	2.550	2.550	2.550	2.550
Z_{oo}/Z	0.414	0.392	0.392	0.392	0.392
Z_1/Z	0.500	0.500	0.6350	0.7407	0.8024
Z_2/Z	1.000	1.000	1.000	0.8696	0.8024
Z_o/Z (Midband)	1	1.0785	1.0785	1.0785	1.0785
Z_s/Z (Midband)	1	0.9272	0.9272	0.9272	0.9272
β (when $Z_s/Z=Z_o/Z$)	90°	90°±30.7°	90°±30.7°	90°±30.7°	90°±30.7°
θ (when $Z_s/Z=Z_o/Z$)	90°	90°±22°	90°±22°	90°±22°	90°±22°

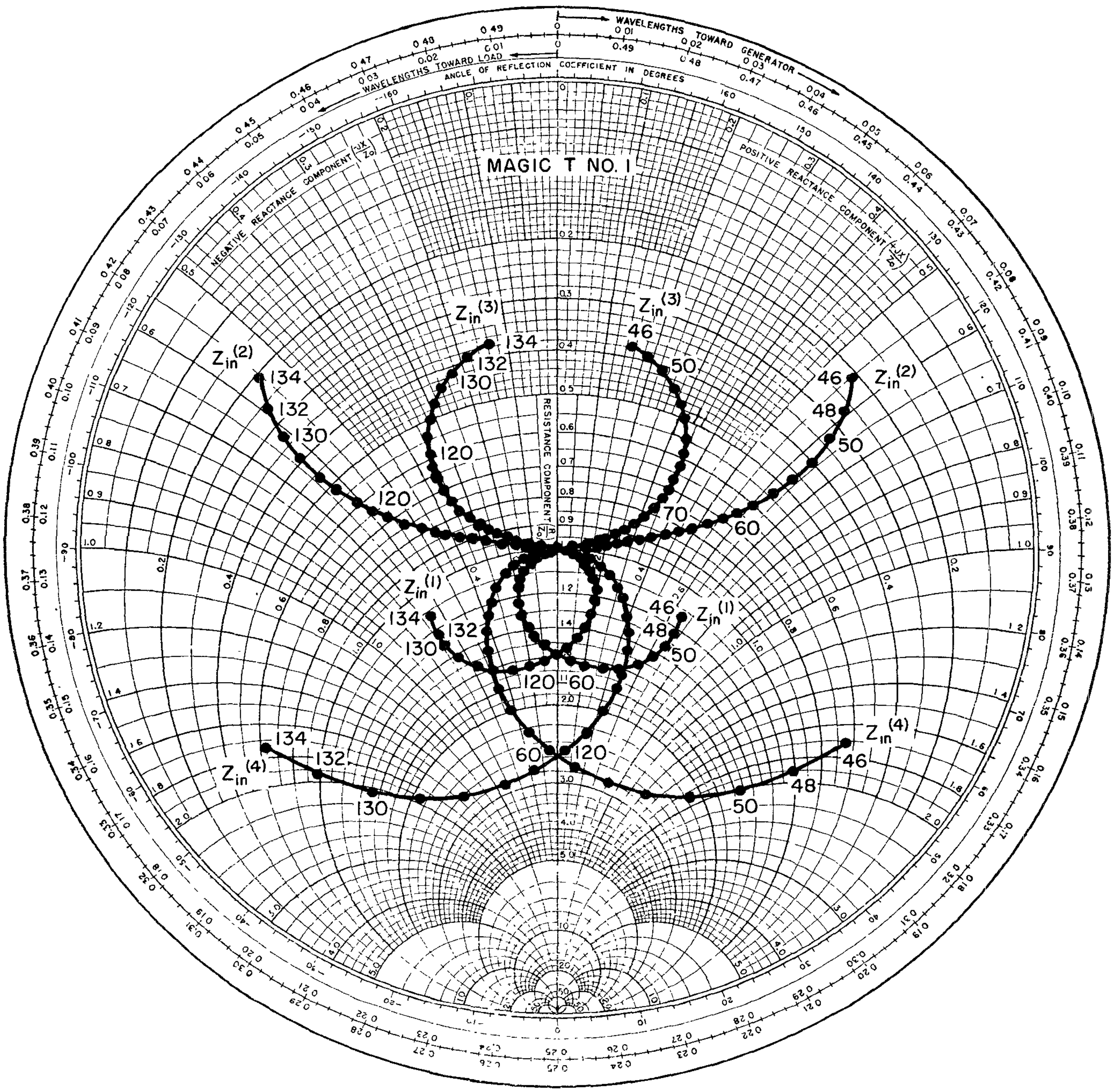

Fig. 5—Input impedance of Magic-T 1.

quency since this device has no electrical plane of symmetry.

Magic-T 1 is designed to be matched at all ports at midband. It also has infinite isolation between ports 1 and 4 and ports 2 and 3 at midband. The input match at the various ports deteriorates at frequencies above and below midband. At the edges of a 2:1 frequency band the VSWR at port 4 rises to 2.55.

Magic-T 2 was designed to have perfect isolation between ports 1 and 4 at $\theta=90°\pm22°$ and approximately equal isolation between these ports at the center and at the edges of a 2:1 frequency band. As mentioned before, it also has perfect isolation between ports 2 and 3 at $\theta=90°$. The frequency variation of the isolation between these pairs of ports is shown in Fig. 10. It is observed that over a 2:1 frequency band the isolation between ports 1 and 4 is always greater than 24.8 db, while the isolation between ports 2 and 3 drops to 22.2 db at the edges of such a band. The input impedance of the various ports is quite similar to that of Magic-T 1, and at the edges of a 2:1 frequency band the VSWR at port 4 rises to 2.45.

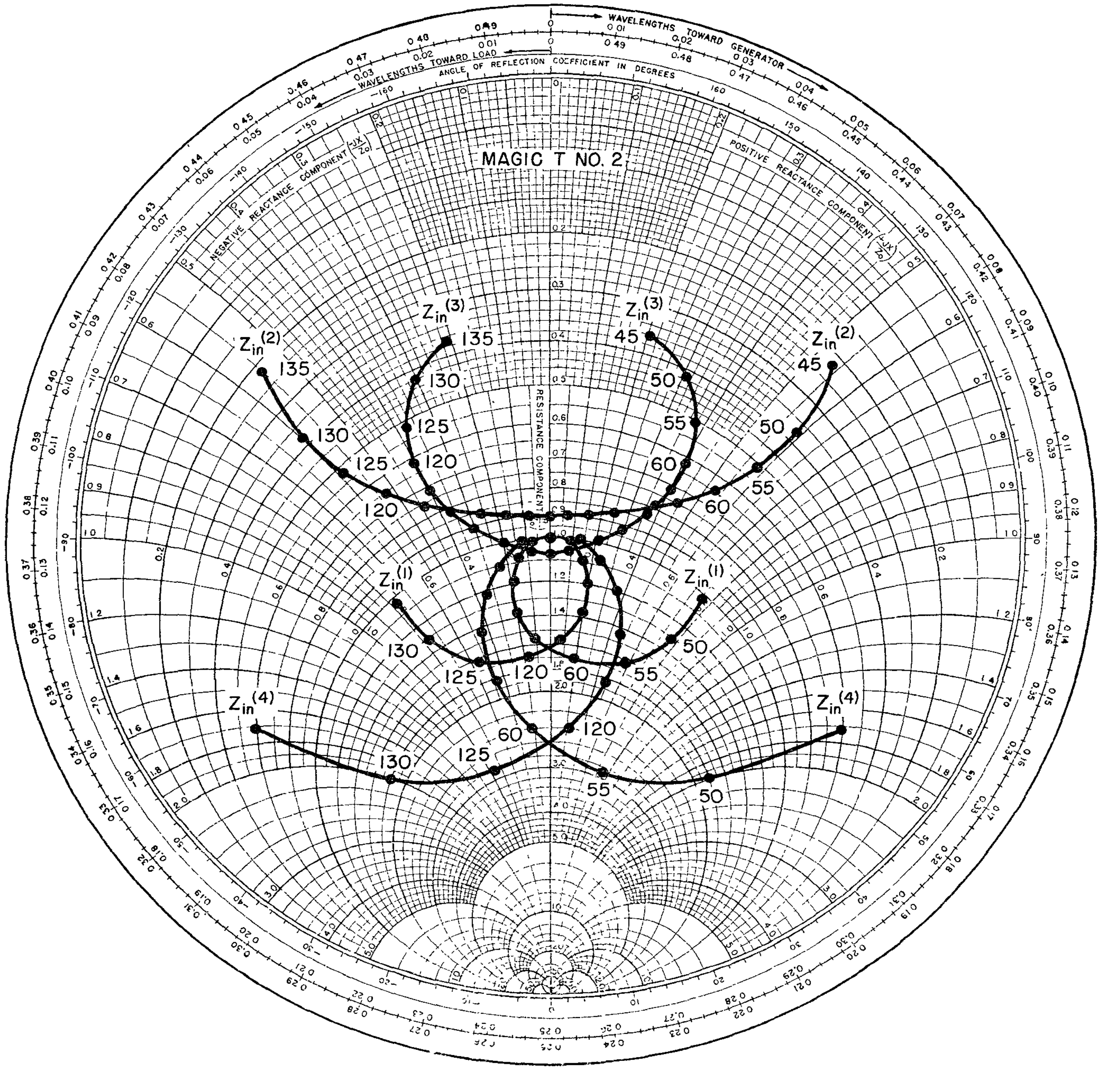

Fig. 6—Input impedance of Magic-T 2.

The internal structure of Magic-T 3 is the same as that of Magic-T 2; however, the terminating impedance Z_1 at ports 1 and 4 has been changed to improve the match at these ports. The input impedance of this Magic-T is shown in Fig. 7. The VSWR at the various ports of this filter is less at the edges of a 2:1 band than in Magic-T 2. The highest VSWR at the edge of the band is 1.93 measured at port 4.

The internal structure of Magic-T 4 is the same as that of Magic-T's 2 and 3. The impedances Z_1 and Z_2 have been chosen to give a perfect match at port 1 when $\theta = 90° \pm 22°$. The input impedance plot of this Magic-T in Fig. 8 shows that this technique considerably improves the match at all ports. The maximum VSWR of 1.58 at the edges of a 2:1 band occurs at port 4.

Magic-T 5 is the same as Magic-T 4, except that it has equal impedances at all the ports whose value is the geometric mean of the values of Z_1 and Z_2 in Magic-T 4. The input impedance of this Magic-T is shown in Fig. 9. Its frequency variation of input impedance is less than that of any of the other Magic-T's. Furthermore, the total impedance excursion at each port as a function of

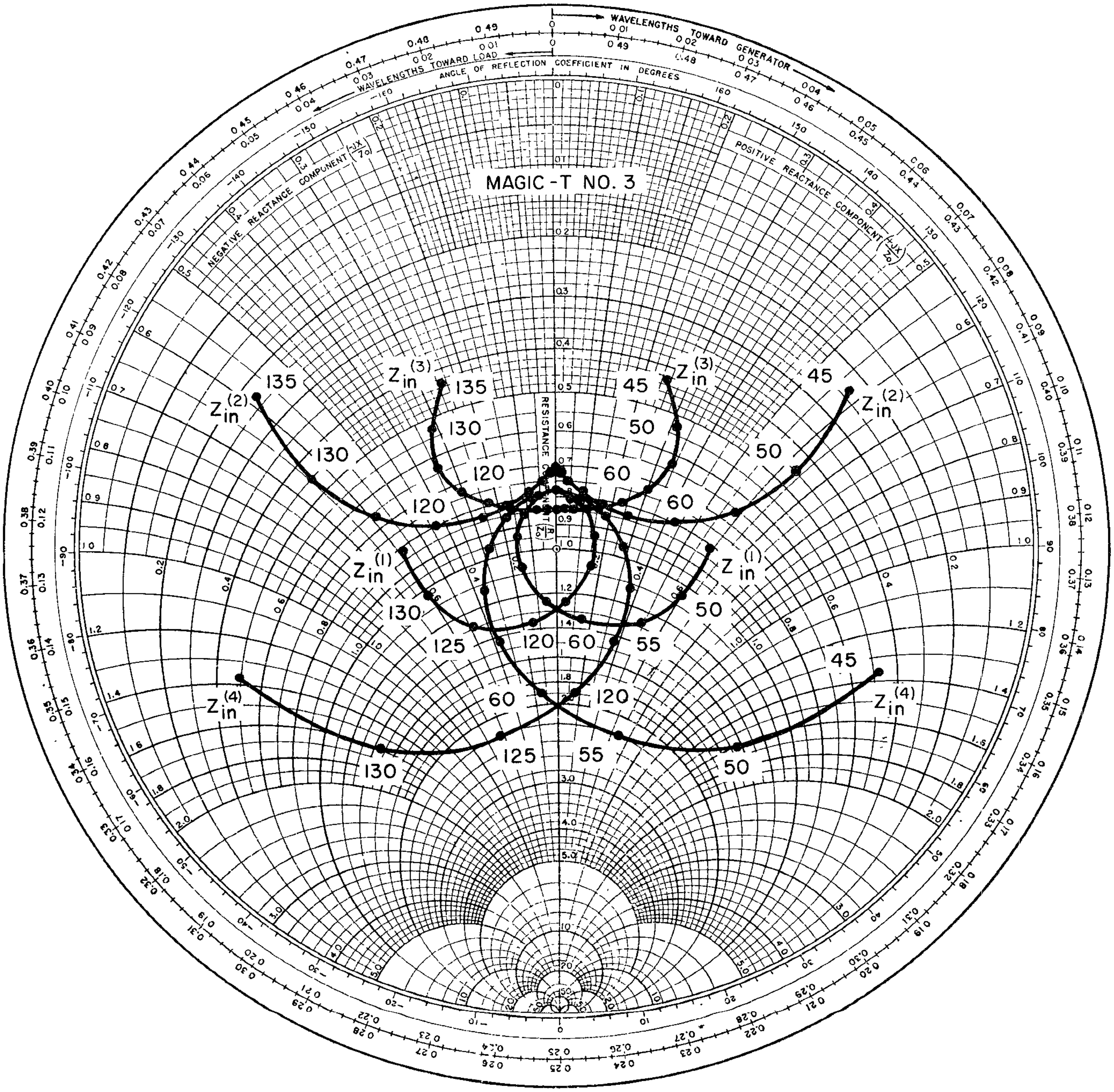

Fig. 7—Input impedance of Magic-T 3.

frequency is quite similar over a 2:1 frequency band. Hence, it is believed that the parameters of Magic-T 5 are essentially optimum for a 2:1 frequency band of operation. The isolation between diagonally opposite ports is plotted in Fig. 10. It is seen that the isolation is quite similar to that of Magic-T 2.

In many applications the most pertinent parameters of a Magic-T are the input impedance of the various ports and the isolation between opposite ports (*i.e.*, between ports 1 and 4 and ports 2 and 3). However, it is sometimes desirable to know approximately the ratio, R, of wanted to unwanted voltages at ports 2 and 3 when port 1 or 4 is energized, or the ratio of wanted to unwanted voltages at ports 1 and 4 when port 2 or 3 is energized. This ratio R is V_b/V_U when port 1 or 3 is energized and V_U/V_b when port 4 or 2 is energized. Here V_b is the balanced voltage and V_U the unbalanced voltage.[8] An approximation to R can be obtained by the

[8] When port 1 or port 4 is energized, $V_b = |V_3 - V_2|/2$ and $V_U = |V_3 + V_2|/2$. When port 2 or port 3 is energized $V_b = |V_1 - V_4|/2$ and $V_U = |V_1 + V_4|/2$.

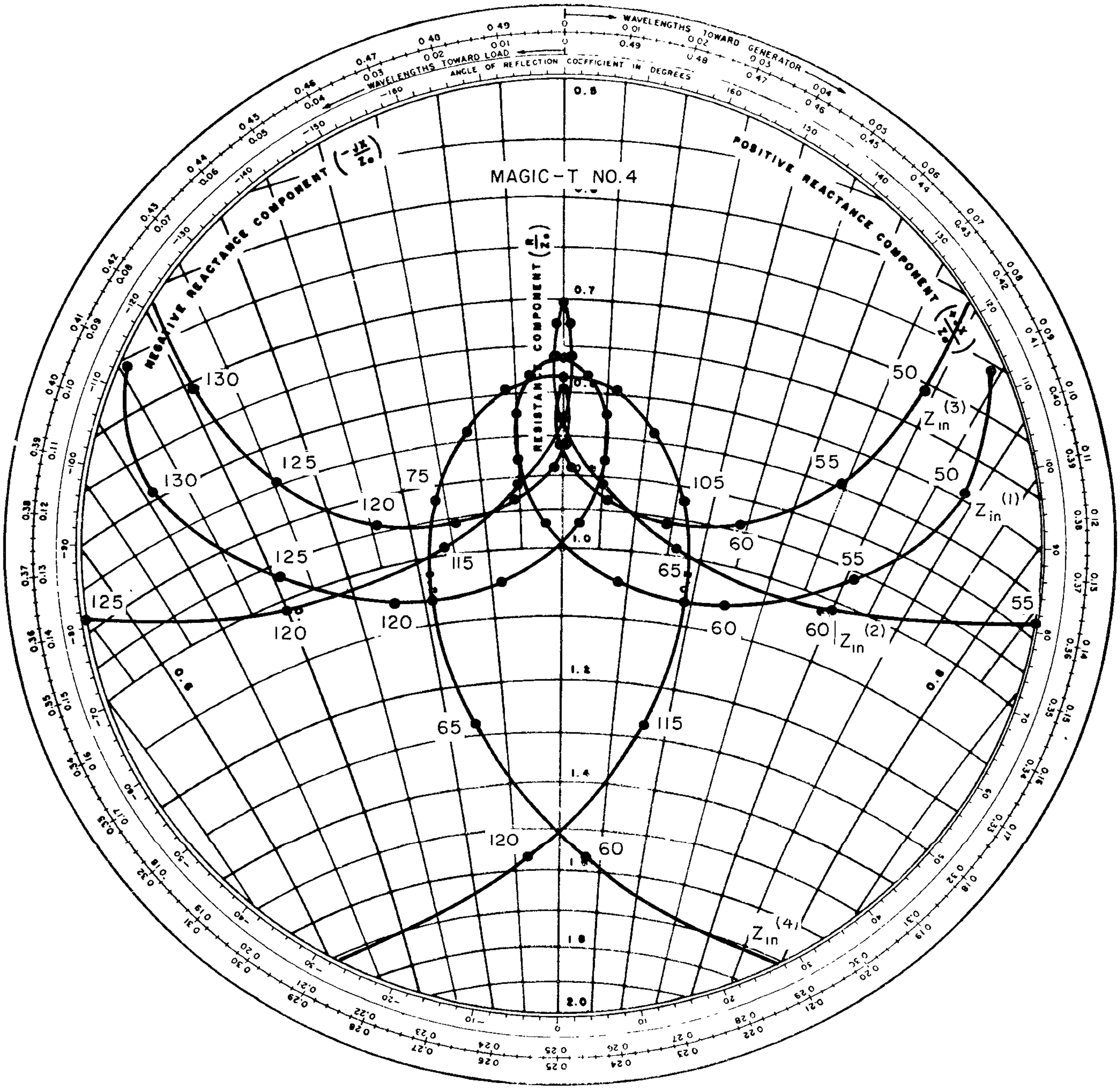

Fig. 8—Input impedance of Magic-T 4.

simple procedure outlined below. Inspection of Fig. 1 shows that when port 1 is energized

$$\frac{V_1^2}{Z_1} \approx \frac{V_2^2}{Z_2} + \frac{V_3^3}{Z_2} + \frac{V_4^2}{Z_1} \tag{15}$$

or

$$\frac{V_1^2}{Z_1} \approx \frac{2V_b^2}{Z_2} + \frac{2V_U^2}{Z_2} + \frac{4Z_1}{Z^2} V_U^2 \cdot \tag{16}$$

In deriving (16), use has been made of the fact that

$$V_2^2 + V_3^2 \equiv 2V_U^2 + 2V_b^2$$

and it is assumed that $\theta \approx \beta = \pi/2$ and $Z_s \approx Z_0 \approx Z$ over the operating band. Recalling that the insertion loss ($I.L.$) is approximately V_1^2/V_4^2 it is seen that

$$\frac{V_1^2}{V_4^2} \approx I.L. \approx \frac{V_b^2 Z^2}{2V_U^2 Z_1 Z_2} + \frac{1}{2Z_1 Z_2} + 1 \approx \frac{V_b^2 Z^2}{2V_U^2 Z_1 Z_2} \tag{17}$$

and

$$R^2 \approx I.L.\left(\frac{2Z_1 Z_2}{Z^2}\right) \cdot \tag{18}$$

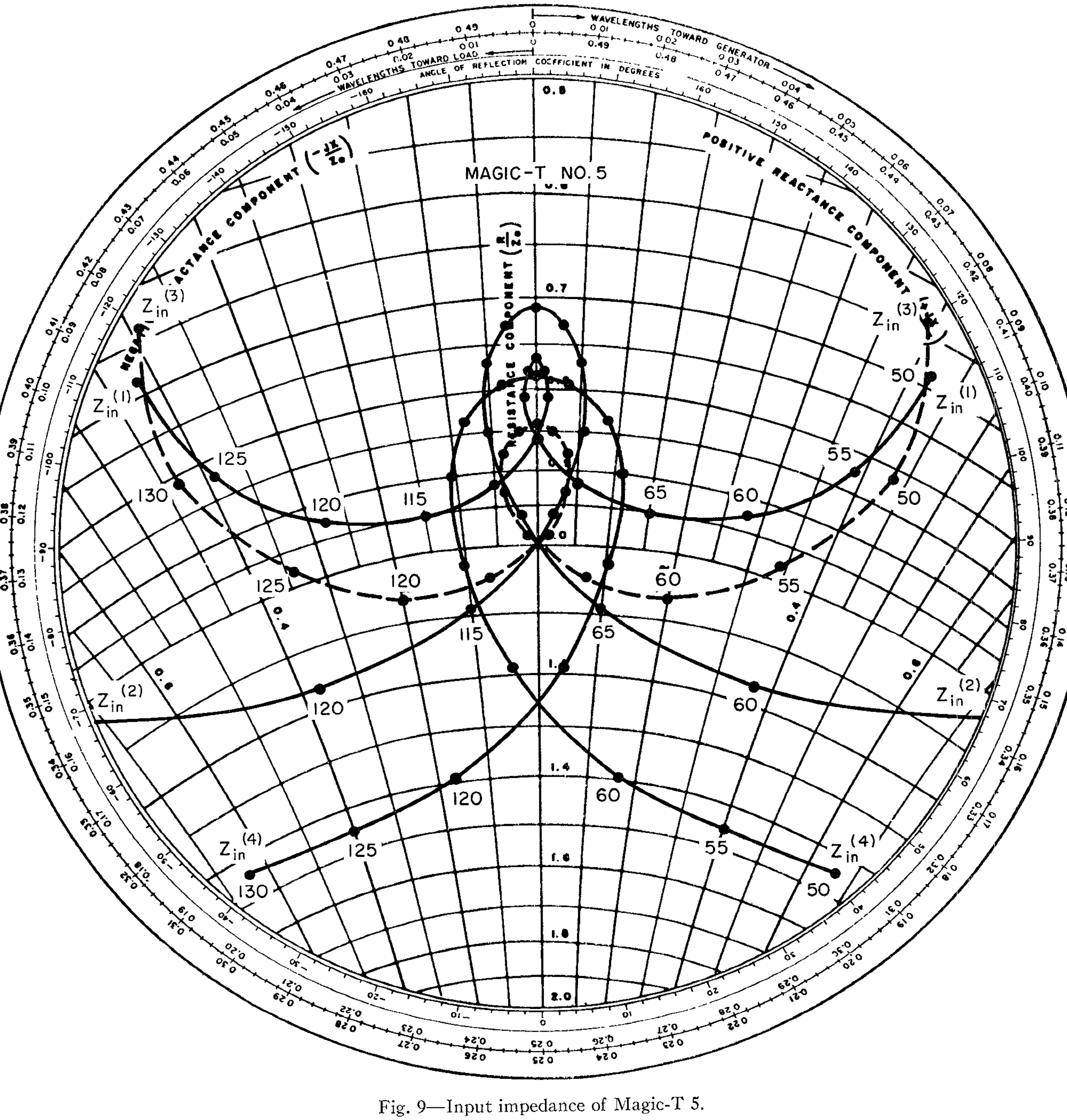

Fig. 9—Input impedance of Magic-T 5.

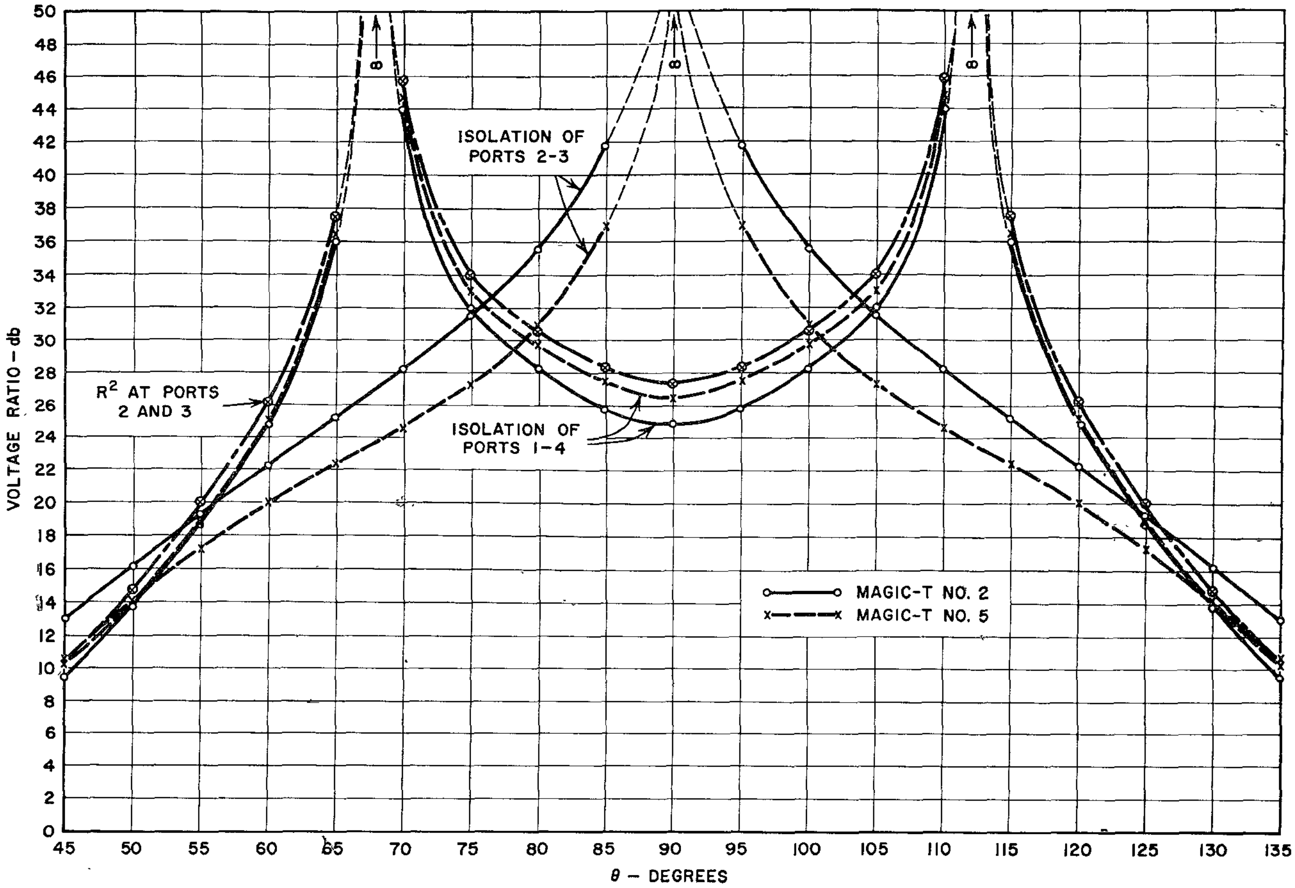

Fig. 10—Isolation between ports 1 and 4 and between ports 2 and 3 for Magic-T's 2 and 5.

It is easy to show that (18) also applies to ports 2 and 3 when port 4 is energized, and to ports 1 and 4 when either port 2 or port 3 is energized.

Application of (18) to Magic-T 2 shows that the insertion loss between opposite ports is numerically equal to R^2 at the other two ports. In Fig. 10 is plotted the correct value of R^2, calculated from (12) and (14) at ports 2 and 3 when port 1 is energized. It is seen to agree very closely with the approximate value of R^2 computed by (18). In Magic-T 5, (18) predicts that R^2 is about 1 db greater than the insertion loss between opposite ports.

Acknowledgment

The author wishes to acknowledge the help of J. K. Shimizu in carrying through some of the theoretical calculations presented here.